

DOMINANT INFLUENCE OF ELECTRON INERTIA
ON ION CYCLOTRON-WAVE GENERATION IN PLASMA

J. C. Hosea and R. M. Sinclair

Plasma Physics Laboratory, Princeton University, Princeton, New Jersey 08540
(Received 27 March 1969)

Electron inertia is predicted to have a dominant influence on ion cyclotron-wave propagation as the wave frequency approaches the ion cyclotron frequency. This influence should effect a reduction in the Stix coil coupling to a plasma column as the plasma density is lowered. Experimental coupling measurements, taken over an appropriate range of plasma density (2×10^{10} to 2.8×10^{12} cm⁻³) on the Model-C stellarator, demonstrate the validity of the theoretical conclusion.

In this paper we present an extension of the study of ion cyclotron-wave generation to lower densities than previously employed in this laboratory.¹ As the plasma density is reduced, the complete cold-plasma theory developed for the Model-C stellarator ion cyclotron-resonance heating (ICRH) system² predicts an increasing effect of electron inertia on such observables as the loading of the Stix coil. We have previously shown^{1,2} good agreement between this theory and experiment for densities $\geq 2 \times 10^{12}$ cm⁻³, where the effects of electron inertia on coil loading (normally neglected) are not dominant. We now extend the comparison of theory and experiment to a lower density range (2×10^{10} to 2.8×10^{12} cm⁻³), where these effects are predicted to become dominant, and continue to find good agreement. Moreover, the measured power coupling normalized to the plasma density actually increases as the density decreases, despite the reduction in coupling caused by the electron inertia. This encourages the use of ICRH³ to heat the ions of low-density plasmas.

The cold-plasma theory of ion cyclotron-wave generation developed by Stix⁴ assumes that electron inertia may be neglected for frequencies ω less than the ion cyclotron frequency $\Omega = Z_i e B_0 / m_i c$, provided that $\omega^2 \ll \Pi_e^2 = 4\pi n e^2 / m_e$ where Π_e is the electron plasma frequency. For the density range quoted above, Π_e^2 / ω^2 ranges from 1.5×10^3 to 3×10^5 , amply satisfying this requirement. However, the complete cold-plasma theory,^{2,5} including the effects of finite electron mass, shows that the optimum loading of the induction coil by ion cyclotron-wave generation should decrease with density for $\Pi_e^2 / \omega^2 \leq 10^5$, in contrast to the prediction of the approximate theory that the optimum loading should increase as the density is reduced. This prediction of the complete theory, which will be ascribed to the strong influence of electron inertia on the general propagation char-

acteristics of ion cyclotron waves, prompted the experiments to be described herein.

Figure 1(a) presents the model used to represent the C stellarator coil system for the theoretical analysis.² A cold, homogeneous plasma column of radius p is immersed in a constant magnetic field B_0 and is surrounded by an induction coil represented by four pairs of filamentary currents $I_0 e^{-i(\omega t)}$ at $r = s$. A Faraday shield and

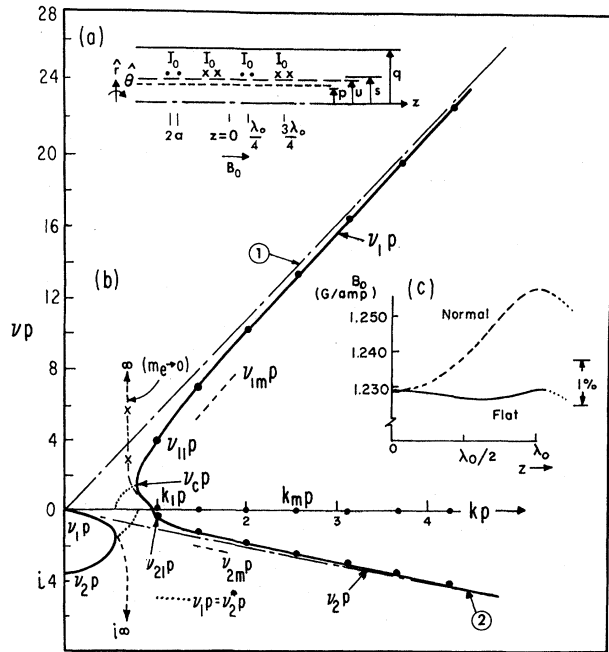


FIG. 1. (a) Coil-system model assumed in the theory. Model-C parameters: $q = 22.3$ cm, $s = 11.5$ cm, $u = 9.0$ cm, $p \sim 6.1$ cm (variable), $\lambda_0 = 38.1$ cm, $k_0 p = 2\pi p / \lambda_0 \sim 1$, $2a = 6.3$ cm, and $f_{rf} = 25$ MHz. (b) $v_1 p$ and $v_2 p$ solutions of the cold-plasma dispersion relation versus kp for a D⁺ plasma of density 10^{11} cm⁻³ and $\Omega = 0.996$. [Also shown is the approximate ($m_e \rightarrow 0$) solution.] Slow-branch asymptotes: ①, Eq. (2); ②, $v_2 p \rightarrow ikp$. Natural-mode wave numbers are indicated for $p = 6.1$ cm. (c) Axial variation of confining field (on axis) over the Stix coil.

shield can (cylindrical waveguide) are at $r = u$ and q , respectively. This model contains all of the characterizing features of the C stellarator system. Furthermore, it provides a theory which is easily adapted to describe cold-plasma wave generation in a plasma column for any θ -independent system.²

The E_θ field of the m th natural mode inside the plasma column is given in terms of Bessel functions by²

$$E_{\theta m} = a_m J_1(\nu_{1m} r) + b_m J_1(\nu_{2m} r), \quad (1)$$

where ν_{1m} and ν_{2m} are the radial wave numbers of the k_m mode which satisfy the plasma dispersion relation [Eq. (1.21) of Ref. 4] and the system dispersion relation $\Gamma = 0$ (Ref. 2) stipulated by the boundary conditions of the model in Fig. 1(a). The constants a_m and b_m are inversely proportional to Γ .⁶ Equation (1) demonstrates the influence of the plasma and system dispersion relations on the natural mode solutions. (It is the extension of E_θ to $r = s$ which is driven by the filamentary coil currents.) The solutions of the plasma dispersion relation, $\nu_1 p$ and $\nu_2 p$, are plotted versus kp in Fig. 1(b). There, $\nu_{1m} p$ and $\nu_{2m} p$, which also satisfy $\Gamma = 0$ at $k_m p$, are indicated by points on the "slow branch" formed by the $\nu_1 p$ and $\nu_2 p$ solutions. Figure 1(b) is calculated for a D⁺ plasma of density 10^{11} cm^{-3} and $\Omega \equiv \omega/\Omega_i = 0.996$, parameters typical of the experimental results to be described.

In Fig. 1(b) we see why the approximate theory (neglecting the electron inertia) is invalid at lower densities even though Π_e^2/ω^2 is large. The solution $\nu_1 p$ is limited by the asymptote

$$\nu_1 p \rightarrow [-P/S]^{1/2} kp \quad (2)$$

which is approximately $[\mu(1-\Omega^2)/\Omega^2]^{1/2} kp$ for $\Pi_e^2/\omega^2 \gg 1$. P and S are terms of the plasma dielectric tensor⁴ and $\mu = m_i/m_e$. As density decreases, detectable ion-wave generation occurs very near $\Omega = 1$. Therefore, the assumption of the approximate theory that $|P/S| \rightarrow \infty$ [see Fig. 1(b)] is not applicable. At sufficiently low densities, all of the natural modes of the approximate theory have radial wave numbers [x of Fig. 1(b)] which are greater than the value $\nu_c P$ where the solutions $\nu_1 p$ and $\nu_2 p$ coalesce, and are simply mathematical artifacts. This result is entirely attributable to the plasma properties and implies that the E_z field of these plasma waves cannot be neglected. (In fact, numerical calculations show that the maximum amplitude of E_z is greater than that of E_θ when $\Pi_e^2/\omega^2 < 10^5$ and becomes

comparable with that of E_r at lowest densities considered here.)

The power transfer, P , from the Stix coil to the excited natural modes propagating along the plasma column is expressed in terms of an equivalent resistance^{1,2}

$$R = P/8I_0^2. \quad (3)$$

The calculated values of $R(\Omega)$ for a given density exhibit a resonance in Ω with a width decreasing with density. The narrowness of this resonance led us to reduce the axial variation of the static confining magnetic field over the length of the Stix coil before making the measurements described below. Figure 1(c) contrasts the best "flat" field achieved ($\pm 0.1\%$) with the $\pm 1.1\%$ "normal" profile.^{1,2} Experimental Ω values, $\bar{\Omega}$, are calculated from the computed field profile, averaged over the length of the coil ($2\lambda_0$), and the measured current in the field coils.⁷

Experimental measurements of R_L defined by $R_L = P_t/8I_0^2 = R + R_c$, where P_t is the total power supplied to the coil system and $R_c (= 0.05 \Omega)$ represents the Ohmic losses not attributable to the plasma, were obtained for D⁺ plasmas as outlined for the low-power experiments in Ref. 1. In order to cover a wide range of density, two methods of plasma formation were used: (i) The breakdown oscillator partially ionized a low gas pressure, and measurements were made in the afterglow. (ii) An Ohmic heating current following the breakdown oscillator completed the ionization; measurements made while the current flowed were for higher densities than those of method (i).^{1,8}

In Fig. 2(a) is shown the dependence of R_L on $\bar{\Omega}$ for various plasma densities measured for a particular flat field profile ($\pm 0.2\%$). The values of $R(\Omega)$ calculated from the complete cold-plasma theory (which neglects the field variation) have added to them the measured value of R_c . The theoretical curves of Fig. 2(a) have been shifted by 0.1% in $\bar{\Omega}$ to give a best fit to the 10^{11}-cm^{-3} data. [The resistance of the current shunt is presently known to within $\pm 0.25\%$. The meter system⁷ used to measure the voltage across the shunt has an absolute accuracy of $\pm 0.1\%$. The relative determination of $\bar{\Omega}$ during the course of one day is clearly better than 0.05% .] For one value of density, theoretical curves obtained with two values of plasma radius are contrasted. We stress that there are no further adjustable parameters and that the agreement between theory and experiment in Fig. 2(a) is absolute.

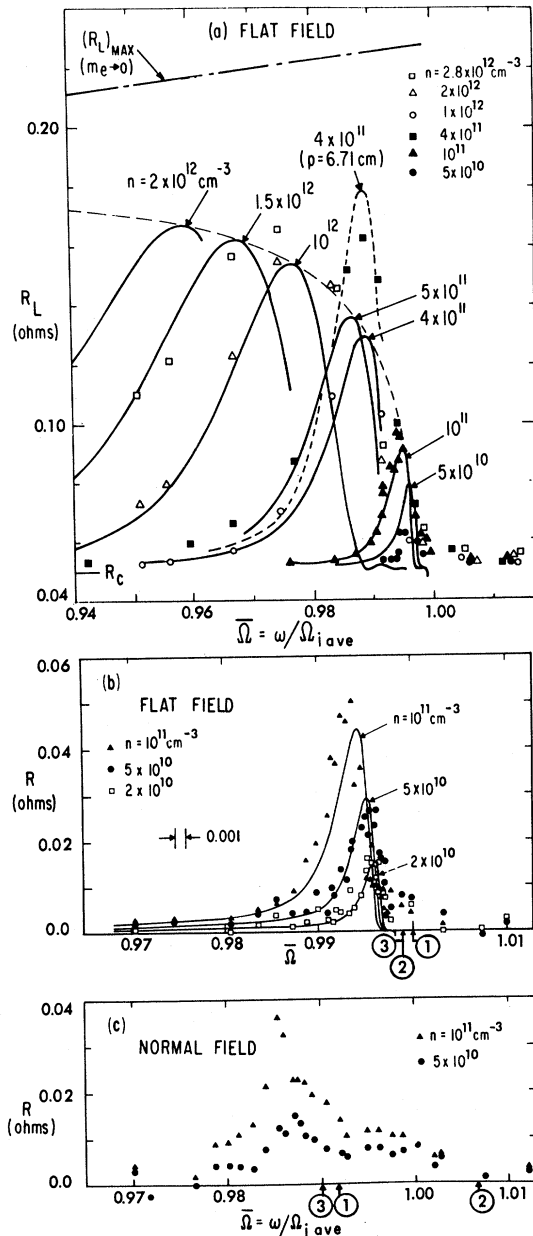


FIG. 2. Comparison of the measured coil loading (R_L or $R = R_L - R_c$ points) with that predicted by the complete cold-plasma theory (curves) for a D^+ plasma [$p = 6.1 \text{ cm}$ (divertor aperture), $T_e = 2.5\text{--}5 \text{ eV}$]. For the theory $p = 6.1 \text{ cm}$ (except where indicated), and $\bar{\Omega}$ is shifted slightly relative to the experimental value $\bar{\Omega}$. (a) Both breakdown-oscillator (solid points) and Ohmic-heating (open points) data are presented for $\pm 0.2\%$ flat confining-field profile ($P_{\text{rf}} = 8 \text{ W}$, $D_2 \ 4 \times 10^{-6}$ and $4 \times 10^{-5} \text{ Torr}$). Theoretical loci of $(R_L)_{\text{MAX}}$ are given including and neglecting electron inertia. (b), (c) Breakdown-oscillator plasma data for the field profiles of Fig. 1(c) ($P_{\text{rf}} = 1 \text{ W}$, $D_2 \ 4 \times 10^{-6} \text{ Torr}$). $\bar{\Omega}$ values for which $\Omega = 1$ at ①, the inner coils, ②, the outer coils, and ③, the minimum field position, are noted.

The high-density ($4 \times 10^{11} \text{ cm}^{-3}$) data obtained for method (i) above at the start of the afterglow are best fitted by a radius somewhat ($\sim 7\%$) larger than that of the divertor aperture. At the lowest density used ($5 \times 10^{10} \text{ cm}^{-3}$), the predicted half-width of the resonance curve is narrower than the variation of the confining field along the coil; this and the lack of data in the vicinity of maximum loading preclude an absolute comparison. The data obtained for method (ii) [Ohmic heating] are best fitted by theoretical curves calculated for half the measured density (this discrepancy was noted previously^{1,2}), while those obtained for method (i) are fitted using the measured density. (The density is measured with an 8-mm interferometer, assuming a uniform radial density profile.) Subsequent studies have shown that the breakdown-oscillator-produced plasma has a nearly square radial density profile, while the plasma carrying Ohmic heating current has a parabolic profile. This corroborates the explanation for the discrepancy given earlier,^{1,2,5} that the experimental mean volume density should be used for the corresponding theory.

The agreement between theory and experiment, both in magnitude and $\bar{\Omega}$ dependence of R_L , is quite satisfactory at the lower densities employed. At the higher densities, the measured $(R_L)_{\text{MAX}}$ follow closely the envelope of the theoretical curves, and the data (when characterized by the mean volume density) agree with theory for values of $\bar{\Omega}$ less than that corresponding to $(R_L)_{\text{MAX}}$. The enhanced loading at higher $\bar{\Omega}$ has been commented on earlier.^{1,2} The envelope for the approximate theory clearly diverges increasingly from the data at low densities.

Additional data, obtained in the breakdown-oscillator-plasma regime (i), are presented in Figs. 2(b) and 2(c) for the flat field and the normal field profiles of Fig. 1(c). The considerable number of experimental $R = R_L - R_c$ data points resolve the resonance curves down to the lowest density considered ($2 \times 10^{10} \text{ cm}^{-3}$). Figure 2(b) complements Fig. 2(a) in the low-density range and shows very good agreement between the complete theory and experiment. [Again, the shift (-0.18%) of the theoretical curves in $\bar{\Omega}$ is consistent with the possible absolute inaccuracy in the confining field measurements.] The second peak in R in the vicinity of $\bar{\Omega} = 1$ is most likely attributable to the direct propulsion of resonant ions by the vacuum fields of the coil (case I of Ref. 3).

The data of Fig. 2(c) clearly demonstrate the

effect of the field variation on ion cyclotron-wave generation. The maximum R is reduced from that of the flat field case and is shifted to lower $\bar{\Omega}$. This behavior is correlated to the $\bar{\Omega}$'s for which $\Omega=1$ at ①, the inner coil; ②, the outer coil; and ③, the minimum field planes. The minimum field value is of particular importance since larger $\bar{\Omega}$'s produce resonance zones under the coil which set up a forbidden axial region for the propagating ion cyclotron waves. The maximum R is attributable mostly to wave excitation by the inner coils; the outer coil excitation is seriously hampered by the forbidden region.

In Fig. 3 we illustrate the asymptotic nature of the value of $\bar{\Omega}$ required for optimum coupling at a given density as density is decreased:

$$\bar{\Omega} \rightarrow \left\{ \frac{\mu}{\mu + (3.83/k_0 p)^2} \right\}^{1/2} \approx 1 - \left(\frac{3.83}{k_0 p} \right)^2 (2\mu)^{-1} \quad (4)$$

instead of tending to unity as predicted by the approximate theory. The experimental maxima of Fig. 2(b) are found to agree with this prediction.

In conclusion, it has been demonstrated that the inclusion of the effects of electron inertia in the cold-plasma theory yields good agreement with the measurements on Model C. This is the first experimental verification of the dominant role of these effects in ion cyclotron-wave propagation.

The results of this study show that sufficient coupling is obtained at low densities to permit appreciable heating of the plasma by wave absorption at a beach. Such heating has yet to be measured, but it seems probable that considerable heating will ensue at moderate power levels; the potential power per ion (for a given I_0) is predicted to increase with decreasing density (R_{\max}/n of Fig. 3). It is necessary, however, to achieve the proper degree of axial field uniformity. A first attempt to heat the ions of low-density plasma⁹ was inconclusive; possibly because the ions were overdriven at the ~ 1 -MW rf power level employed, and because the axial confining-field profile was "normal" [Fig. 1(c)].

It is further suggested that the ion cyclotron loading resonance at low density can provide a calibration of confining-field measurement systems to an accuracy commensurate with the field variation over the coil. [The Model-C system used to measure confining-field current⁷ is seen to provide relative measurements to better than ~ 10 A out of 25 kA [Fig. 2(b)], but appears to overestimate the magnitude of the field current by $\sim 0.15\%$ suggesting that the resistance of the

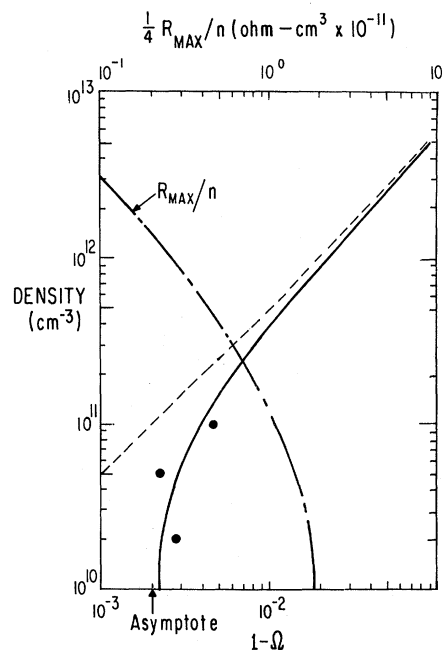


FIG. 3. Theoretical $\bar{\Omega}$ for optimum coupling as a function of density, for a D^+ plasma with $p=6.1$ cm, including (solid curve) and neglecting (dashed curve) the effects of electron inertia. The points indicate the position of the measured R_{\max} in Fig. 2(b). [The experimental values of $\bar{\Omega}$ were increased by 0.0018 before locating them on the abscissa, corresponding to the same correction as in Fig. 2(b).] Also shown is the potential power per particle [R_{\max}/n] normalized to unit current in the Stix coil.

shunt is that much greater than its nominal value.] Also, measurements of $R_L(\bar{\Omega})$ at low rf power can serve as a mass spectrometer to measure the density of resonant ions. In a one-ion plasma, a measure of $\bar{\Omega}$ for $(R_L)_{\max}$ is sufficient at high densities, while below 10^{11} cm^{-3} a single value of $\bar{\Omega}$ can be used, and $(R_L)_{\max}$ measured continuously during a discharge. In a two-ion plasma (e.g., deuterium plus impurities), theoretical calculations show that the value of $(R_L)_{\max}$ is given predominantly by the total ion density (= the electron density), while the width and $\bar{\Omega}$ of the resonance depend principally on the density of resonant ions. Thus, it would be easy to determine if the resonant ions in a plasma were being lost at a much faster rate than the impurity ions.

We would like to express our appreciation to Professor T. H. Stix and to Dr. D. J. Grove for their continued encouragement and interest. We would also like to thank A. J. Sivo, C. Bushnell, and J. M. Perron and the Model-C stellarator operating staff for their help.

¹M. A. Rothman, R. M. Sinclair, I. G. Brown, and J. C. Hosea, Princeton Plasma Physics Laboratory Report No. MATT-606, 1968 (to be published).

²J. C. Hosea and R. M. Sinclair, Princeton Plasma Physics Laboratory Report No. MATT-673, 1969 (to be published).

³T. H. Stix, *Phys. Fluids* **1**, 308 (1958).

⁴T. H. Stix, *The Theory of Plasma Waves* (McGraw-Hill Book Company, Inc., New York, 1962), Chaps. 1-5.

⁵D. R. Sigman and J. J. Reinmann, National Aeronautics and Space Administration Technical Note No. TN D-4058, 1967 (unpublished).

⁶This formalism for the natural-mode E_θ field parallels that given by Stix in the approximate theory [Ref.

4, Sec. 5-4, in which $\Gamma = kpJ_1(\nu p)K_1'(kp) - \nu pJ_1'(\nu p)K_1(kp)$].

⁷J. W. Spinner, in *Proceedings of the Symposium on Engineering Problems of Controlled Thermonuclear Research, Livermore, California, 4-7 May 1965* (Clearing House for Scientific and Technical Information, Washington, D. C., 1965), pp. 100-105.

⁸R. M. Sinclair, S. Yoshikawa, W. L. Harries, K. M. Young, K. E. Weimer, and J. L. Johnson, *Phys. Fluids* **8**, 118 (1965).

⁹I. G. Brown, D. L. Dimock, E. Mazzucato, M. A. Rothman, R. M. Sinclair, and K. M. Young, in *Plasma Physics and Controlled Nuclear Fusion Research* (International Atomic Energy Agency, Vienna, Austria, 1969), Vol. I, p. 497.

MAGNETIC FIELD DEPENDENCE OF LASER EMISSION IN $\text{Pb}_{1-x}\text{Sn}_x\text{Se}$ DIODES*

A. R. Calawa, J. O. Dimmock, T. C. Harman, and I. Melngailis

Lincoln Laboratory, Massachusetts Institute of Technology, Lexington, Massachusetts 02173

(Received 26 May 1969)

The magnetic field dependence of long-wavelength infrared laser emission has been studied in $\text{Pb}_{1-x}\text{Sn}_x\text{Se}$ diodes for compositions in the range $0 \leq x \leq 0.3$. For $x > 0.15$ the energy of the lowest transition decreases with increasing magnetic field whereas for $x < 0.15$ this energy increases. This unique observation is consistent with a theory of magnetic energy levels proposed by Baraff and also strongly supports the inversion model for the energy bands in Pb-Sn chalcogenides.

The temperature dependence of laser emission in $\text{Pb}_{1-x}\text{Sn}_x\text{Se}$ diodes in the composition range $0 \leq x \leq 0.3$ has recently been reported¹ and the magnetic field dependence of laser emission and spontaneous luminescence has been measured for PbS, PbSe, and PbTe² and for low-SnTe-content $\text{Pb}_{1-x}\text{Sn}_x\text{Te}$ diodes.³ We report here the results of measurements made on a number of $\text{Pb}_{1-x}\text{Sn}_x\text{Se}$ diode lasers in the above composition range at magnetic fields up to 145 kG. The results support the model previously proposed⁴ in which the valence- and conduction-band states in $\text{Pb}_{1-x}\text{Sn}_x\text{Se}$ alloys approach each other, invert, and move apart as SnSe is added to PbSe. At low temperatures this inversion occurs at about $x = 0.15$. For the alloys on the SnSe-rich side of the inversion point the lowest energy transition between magnetic levels of the conduction and valence bands has an energy which decreases with increasing magnetic field. To our knowledge this is the first such observation in any material. In addition the results give a direct indication of the effect that the higher lying energy bands have on the conduction and valence-band-edge masses and g factors in these materials.

For the magnetic-field measurements the diodes were near liquid-He temperature and oriented with the diode current parallel to the magnetic field in a $\langle 100 \rangle$ crystallographic direction. The laser radiation was emitted perpendicular to this direction. The photon energy of the laser emission as a function of magnetic field is shown in Fig. 1 for diodes of $\text{Pb}_{1-x}\text{Sn}_x\text{Se}$ with $x = 0, 0.05, \text{ and } 0.10$ and in Fig. 2 for $x = 0.19, 0.22, \text{ and } 0.28$. The Landau levels shown schematically in the insets identify the transitions observed. At low magnetic fields one generally observes the line T_2 . As the field is increased the emission switches to T_1 . If the diode current is increased the T_2 emission persists up to higher magnetic field values and in some cases a third line T_3 is observed. For all of the alloys studied with $x < 0.15$ (including PbSe) the T_1 line is found to have a positive slope, in most cases about 10^{-7} eV/G. For alloys with $x > 0.15$ the slope of this line is negative but has about the same magnitude. The zero-field energy gap as a function of alloy composition is shown in Fig. 3. The mole fraction of SnSe (x) was measured using an electron microprobe, and the energy-gap values were obtained from extrapolations of the magnet-